Engineering Failure Analysis 174 (2025) 109494

Contents lists available at ScienceDirect

Engineering Failure Analysis

journal homepage: www.elsevier.com/locate/engfailanal

Fatigue prediction of wind turbine tower considering the effect of high-tension bolt failure

Yuka Kikuchi, Takeshi Ishihara *

Department of Civil Engineering, School of Engineering, The University of Tokyo, 7-3-1 Hongo, Bunkyo-ku, 113-8656 Tokyo, Japan

ARTICLE INFO

Keywords:
Wind turbine
High-tension bolts
Fatigue failure
FEM analysis
Aerodynamic model
Structural model

ABSTRACT

In this study, an accident at Taikoyama wind farm is investigated by the fatigue analysis of high-tension bolts and tower. Firstly, a sophisticated aeroelastic model is proposed by identifying the structural and control parameters and validated with the measured tower base bending moment. The predicted bending moment at the tower top shows that the tensile stress occurs at the downwind side of tower due to the eccentricity of the centre of gravity of rotor and nacelle. The bolt axial force is then predicted using the finite element model of the tower top with consideration of effects of ball bearings, yaw breaks and pinion gear. The predicted bolt fatigue life is about three months when the residual bolt axial force is less than 30 %, which matches the maintenance record. Finally, the stress of the tower shell is investigated by a sophisticated FEM model. It is found that the tensile stress is generated inside of the tower shell due to the leverage effect. The relationship between the local stress and the nominal stress shows the nonlinearity and the local stress in the case with damaged bolts is three times larger than that in the case with intact bolts. The predicted fatigue life of the tower favourably agrees with the observation.

1. Introduction

On 12th March 2013, the nacelle of Lagaway 750 kW No.3 wind turbine at the Taikoyama wind farm in Japan fell to the ground in normal wind condition about 10 to 15 m/s as shown in Fig. 1 (a). The 46-meter-high tower ruptured almost horizontally near the weld between the top and the wind turbine connection flange as shown in Fig. 1 (b). The Taikoyama wind farm is located north of the top of Taiko Mountain with an elevation of 638.1 m in the northern Kyoto Prefecture as shown in Fig. 1 (c) and the wind turbines were installed along the west-facing ridge as shown in Fig. 1 (d). It has been only 12 years since the start of the operation in November 2001. The accident survey at that time clarified the cause of the accident was that the fatigue failures of high-tension bolts on the tower-top flange accelerated the cumulative damage of tower shell [1]. Wind turbine tower failures are less frequently reported than blade failures. Most wind turbine tower failures occur due to collapse caused by tropical cyclones, and it has been found that these can be prevented by proper design and construction, as recently studied by Lee and Bang [2], and Chou and Tu [3]. Alonso-Martinez et al. [4] described the collapse of a wind turbine tower in 2008, which occurred two months after it was put into operation due to a failure of the lower flange. The collapse of the tower was caused by material defects and design errors in the flange. However, these studies did not quantitatively investigate the fatigue life of the tower. Tran and Lee [5] conducted FEM analysis to investigate the behavior of L-type flange connections in wind turbine towers. However, these studies did not address the mechanism of fatigue failure occurring

* Corresponding author.
E-mail address: ishihara@bridge.t.u-tokyo.ac.jp (T. Ishihara).

https://doi.org/10.1016/j.engfailanal.2025.109494
Received 2 January 2025; Received in revised form 9 February 2025; Accepted 4 March 2025
Available online 4 March 2025

inside the tower shell. The fatigue life of tower as well as mechanism of accident need to be quantitively investigated.

In the accident, 14 out of 60 high-tension bolts on the top flange fractured and fatigue failure occurred at the downwind side of the tower during westerly wind as shown in Fig. 2 (a) and (b), though the tower shell in the downwind side of the turbine is generally subjected to compressive stress [1]. The mechanism of the phenomena needs to be investigated using the aeroelastic wind turbine model. However, the structural and control parameters of the aeroelastic wind turbine model are unknown and need to be identified from the measurement data. Yamaguchi et al. [6,7] identified the structural and control parameters of a pitch-regulated offshore wind turbine from the measured tower moment and power production. Ishihara et al. [8] also identified the structural and control for an active stall regulated onshore wind turbine from the measured tower moment and power production.

The maintenance record of No.3 wind turbine at the Taikoyama wind farm showed that the bolt fatigue failures were observed three times as shown in Table 1. The broken and loose bolts were first discovered and replaced in June 2008 since the wind farm begun operation in October 2001. The bolt integrity had been confirmed in a regular inspection conducted the previous month in May, indicating that the bolt had broken in one month. The second replacement was carried out in February 2012. As in the previous case, the failure was discovered one to two months after the last bolt integrity check. The accident occurred one year after the second failure and two to three months after the last bolt integrity check. In all cases, the bolt failure occurred within three months after the periodic inspection. The accident survey also found that the retorqueing of high-tension bolts were not conducted adequately, which led to the rapid reduction of the residual bolt axial force [9]. The bolt axial force is conventionally calculated by a transfer function between the external load and the load in the bolt [10–12]. Pedersen and Pedersen proposed the simplified expression of the bolt connection stiffness [13] and applied the finite element method with superelements to solve the contact problem with the combination of prestress and external load in an overall non-iterative manner [14]. Kang et al. [15] proposed a solid bolt model, and a simplified bolt model to evaluate the fatigue life of high-strength bolts connected between shaft and hub in a 2.5 MW wind turbine. However, the conventional fatigue analysis does not show such a short fatigue life of the high-tension bolt even with the low residual bolt axial force. Kikuchi and Ishihara [16] built a full flange FEM model and validated it using the measured strain distribution of the tower shell and indicated that the fatigue life of the high-tension bolt needs to be investigated with the full flange FEM model.

The fatigue life of the tower shell of accident wind turbine was much shorter than the designed lifetime of 20 years. The microstructure survey showed that the fatigue failure originated on the inner side of the tower shell due to the complex structure of nacelle. It was suggested that the tower eventually reached fatigue failure after three bolt failure events. From the maintenance record, the total period with damaged bolts was 4 to 6 months and that with intact bolts was 11 years. Schmit [17] investigated the elastostatics behavior of an eccentrically tensioned L-joint with prestressed bolts. Peterson [18], Tobinaga and Ishihara [19]. Seidel et al. [20] investigated the effect of geometrical imperfections on fatigue design of bolted ring flange connections. 3D FEA models including

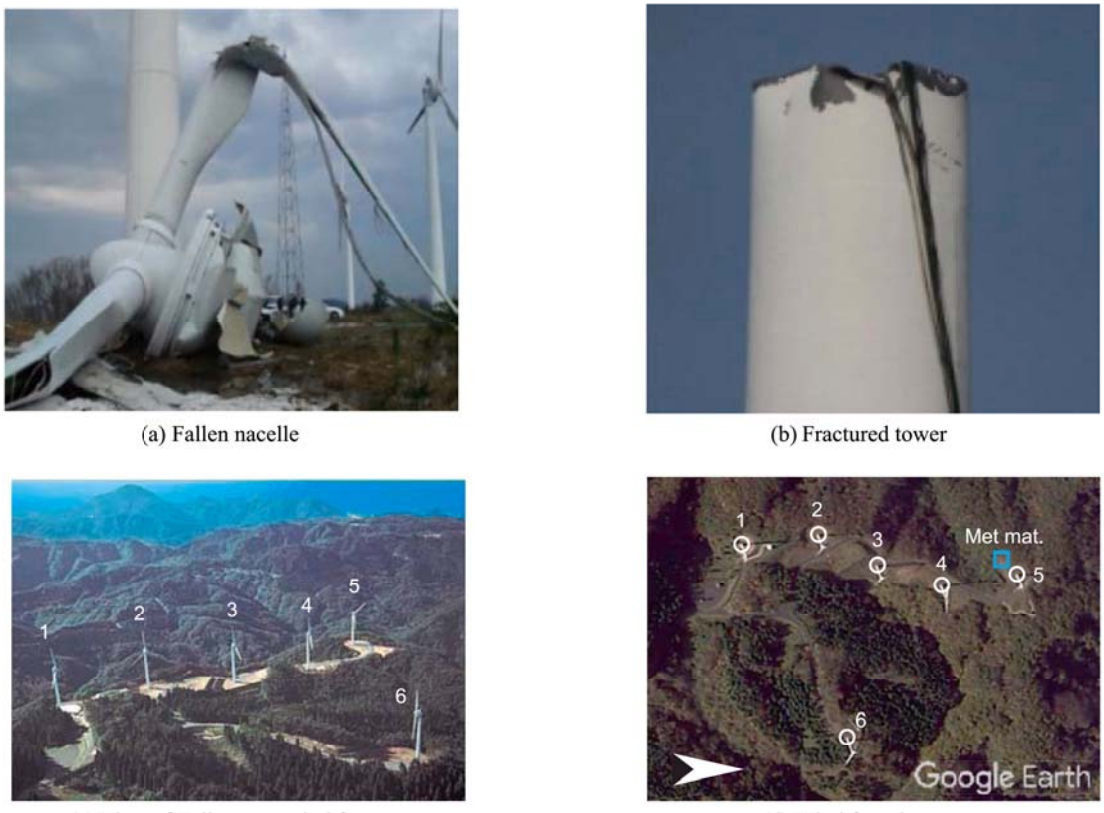

(a) Fallen nacelle

(b) Fractured tower

(c) View of Taikoyama wind farm

(d) Wind farm layout

Fig. 1. Overview of accident at Taikoyama wind farm in Japan.

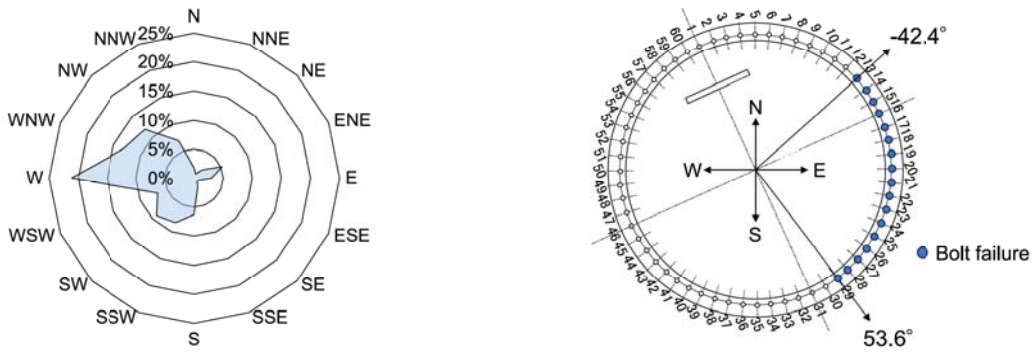

(a) Wind rose (b) Location of failure bolts

Fig. 2. Accident survey of No. 3 wind turbine at Taikoyama wind farm.

Table 1
Maintenance record of bolt failure of No. 3 wind turbine at Taikoyama wind farm.

Maintenance year	Bolt status	Event	Period	
			Damaged bolts	Intact bolts
06/2008	6 bolts failure 17 bolts loosen	Replacement	1 month	6.5 years
02/2012	17 bolts failure	Replacement	1–2 months	3.5 years
03/2013	7 bolts failure 7 bolts loosen	Accident	2–3 months	1 year

geometrical imperfections are validated with the measurement. The short lifetime of the damaged tower needs to be investigated based on the maintenance record.

In this study, the accident is investigated to identify the root cause and understand the key factors to the fatigue life of the bolts and tower shell. An aeroelastic wind turbine model is proposed by identifying the structural and control parameters and a FEM model of tower top structure is built considering the three dimensionality and the nonlinearity of the bolts in section 2. The aeroelastic wind turbine model is then used to clarify why fatigue failure occurs at the downwind side of the turbine. The fatigue life of the high-tension bolt is predicted by the FEM model. The local stress of the tower shell is predicted by the FEM model to clarify why fatigue failure

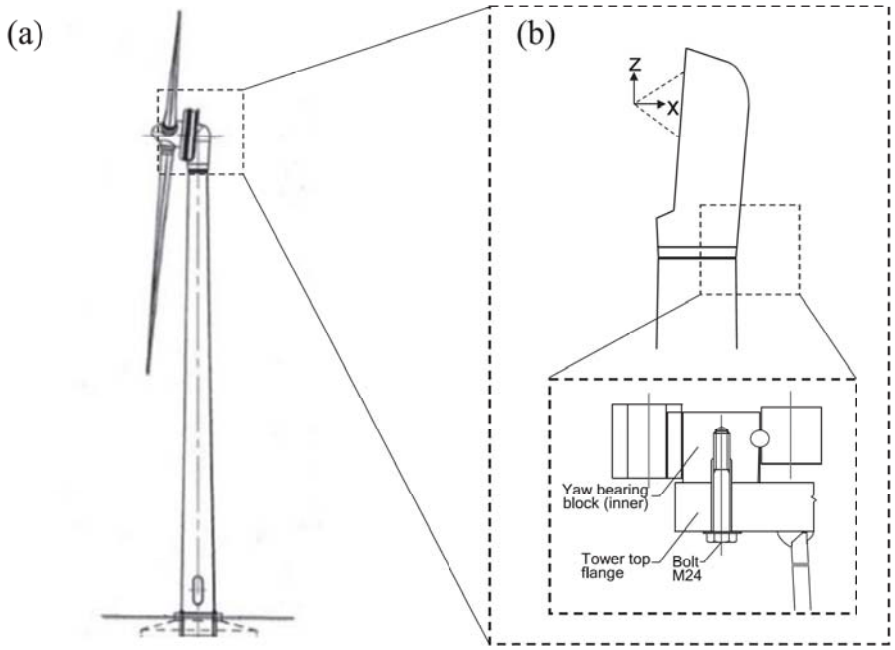

Fig. 3. Numerical models, (a) aeroelastic wind turbine model, (b) 3D FEM nacelle-tower model.

originates inside of tower shell. The fatigue life of tower is predicted using the relationship between the local stress and the nominal stress and compared with the maintenance record in section 3. Conclusions are summarized in section 4.

2. Onsite measurement and numerical models

The onsite measurement conducted at Taikoyama wind farm is described in section 2.1. Fig. 3 illustrates the schematic of aero-elastic wind turbine model and the numerical nacelle-tower model. The aerodynamic model is proposed and validated with measurement data in section 2.2. The FEM models for the flange-bolt and nacelle-tower are described and validated in section 2.3.

2.1. Onsite measurement at Taikoyama wind farm

The comprehensive measurement campaign is conducted on No.1 wind turbine to identify the structural and control parameters and to validate the numerical models. The power, rotor speed and pitch angle data are evaluated from the supervisory control and data acquisition (SCADA) signals of No.1 wind turbine following the instruction of IEC 61400–12 [21]. 10-minute averages of wind speed in 1 m/s bins are collected over the wind turbine's operating range of 4 m/s to 25 m/s.

The onsite wind condition is analysed using the observation mast data from 27/11/2015 to 15/03/2016. Cup anemometers and one vane anemometer have been installed at the three elevations of 40.0 m, 50.0 m, and 59.0 m respectively on the mast. An ultrasonic anemometer has been installed at 59.6 m, on the mast, with a sampling rate of 4 Hz. Fig. 4 (a) depicts Rayleigh distribution fitted to the wind speed measured at each anemometer. The average wind speed at the site is almost 8.5 m/s, which corresponds to IEC class II category [22]. The Rayleigh distribution corresponding to IEC class II favourably agrees with the measurements. Turbulence intensity is calculated from the measurement data. The wind shear is estimated as 0.2 from the vertical wind profile. Fig. 4 (b) plots the estimated turbulence intensity of the 1 m/s bin averaged turbulence intensity and the Normal Turbulence Wind (NTW) for IEC category A. 90 % quantile value of measurements agree well with the NTW model for IEC category A. Here., the wake effect of turbine is not considered since the prevailing wind direction is westerly as shown in Fig. 2 (a) and the wind turbines are aligned in a north–south direction shown in Fig. 1 (d).

Eight strain gauges are installed on the tower shell at 12.6 m above tower base from 02/02/2015 to 28/02/2015 to measure the tower base moment by Eq. (1). The initial offset of the strain gauges is calibrated by using the strain data measured during 360 degrees of the nacelle yaw rotation. The data are sampled at 20 Hz frequency and statistical values, such as mean, maximum and standard deviation are calculated from all the 10-minute time series data.

$$M_{total} = \frac{EI}{d}\sqrt{(\varepsilon_E - \varepsilon_W)^2 + (\varepsilon_S - \varepsilon_N)^2} \tag{1}$$

where M_{total} and ε_i are the moments and strains at corresponding direction, EI is the bending stiffness, d is the inner diameter of tower section at the measurement height.

The forced vibration test is conducted from 14/08/2013 to 16/08/2013 to measure the natural frequency and damping ratio of the wind turbine. A servo accelerator with a sampling frequency of 20 Hz is installed. The natural frequencies of the tower are evaluated using the measured acceleration data, and the damping ratios are estimated using the measured ambient vibration by the random decrement method.

2.2. Aero-elastic model and validation

A sophisticated aeroelastic wind turbine model is built using GH Bladed based on the guideline [23]. The dimensions and wight of

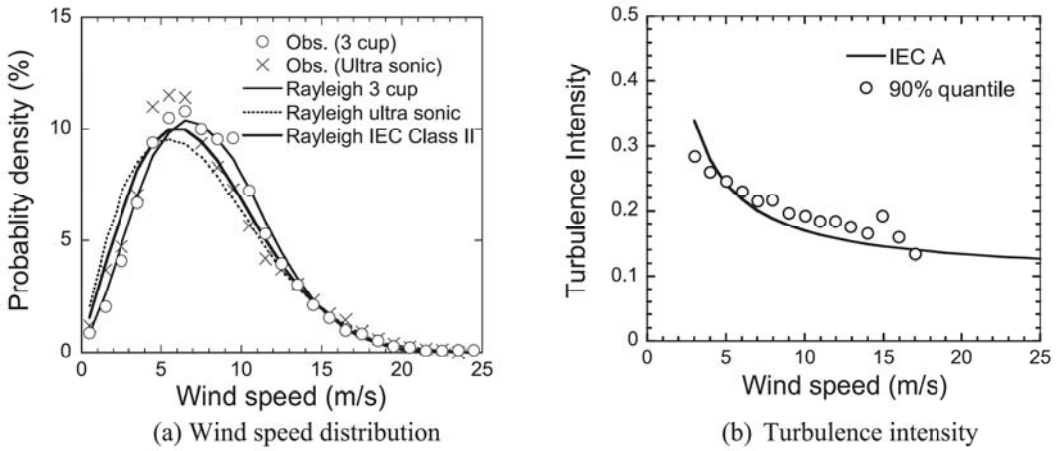

Fig. 4. Observed wind condition.

the nacelle, rotor, hub and tower are shown in Table 2. The aerodynamic properties of the blade are based on NREL models described in Wind Energy Handbook [24]. Blade aerofoils use S818 for root section, S830 for primary section and S831 for tip section. The damping ratio of the first and second tower modes are set as 0.5 % evaluated from the measurements. Table 3 shows the measured and estimated first and second natural frequencies. The errors of the predicted first natural frequencies are less than 2 % in fore-aft and side-side directions.

The wind turbine has a conventional variable speed and a blade pitch-to-feather configuration. The parameters used in the standard PI control are based on the model proposed in Wind Energy Handbook [24] and are shown in Table 4. The rated power of 630 kW and the rotor speed of 26 rpm are identified from the measurement data as shown in Fig. 5. These values are lower than the nominal values, which is used as a countermeasure against overspeed phenomena in high turbulence regions. The proportional gain and integral gain for torque control and those for pitch control are calculated based on the guideline [23]. The gain scheduling follows the methods proposed by Yoshida [25].

The simulation with 35 different random turbulence seeds at each wind speed is conducted based on the measured turbulence intensity I_v/I_u and I_w/I_u of 1.0 and 0.7, and wind shear of 0.2. The Kaimal turbulence model is used in the simulations. Since the power curve and pitch angle using the standard PI control are overestimated as shown in Fig. 6, the mechanical loss and the pitch delay models are introduced in this study. In the mechanical loss model, a total loss of 31.85 % is assumed. In the pitch delay model, a pitch lag of 5 degrees is assumed since a 32 % reduction in lift force coefficient corresponds to a change in the angle of attack of approximately 5 degrees. Both of mechanical loss and pitch delay relatively show a good agreement with measurements, while the standard PI model overestimates the generated power, rotor speed and pitch angle. However, the mechanical loss model overestimates the average of tower base moment, which can be explained the torque balance given by the following equation.

$$J\frac{d\Omega_h}{dt} = \Gamma_{mec} - \Gamma_G - \Gamma_{loss} \tag{2}$$

where Γ_{mec} is the mechanical torque, Γ_G is the electromagnetic torque resulting from the interaction between the stator and rotor fluxes, Ω_h is the high-speed shaft rotational speed, and Γ_{loss} is the torque loss. In order to maintain the electromagnetic torque, the loss of Γ_{loss} is higher and the mechanical torque Γ_{mec} is larger. Therefore, the larger mechanical loss. the larger moment increases. On the other hand, the pitch delay model shows good agreement with the measurements, which reduces both the generator torque and the aerodynamic thrust simultaneously. In conclusion, the pitch delay model is used in this study.

2.3. Numerical nacelle-tower model and validation

A sectional model with solid elements for the bolt connection is first built as same as that by Seidel and Schaumann [26] as shown in Fig. 7 (a). M36 bolt is used with the nominal diameter of 36 mm. The top of upper flange is forced to displace in 1 mm, which corresponds to 310 kN force applied in Seidel and Schaumann [26]. The boundary condition of the top of lower flange is a rolling constraint. The surfaces of the flange, washer and bolt are defined as a contact surface with the friction factor of 0.2. The screw threads between the male and female threads are not taken into account. The pretension of 485 kN is loaded with increments on the bolts in the vertical direction. Density is 7850 kg/m3, Poisson's ratio is 0.3 and Young's modulus is 206000 MPa. Typical elastic and plastic behaviour of steel are used for flanges, bolts and tower shell in the FEM analysis as shown in Tobinaga and Ishihara [19], while the loading is in the elastic region during the power production.

A model with beam element for bolt connection is then built as shown in Fig. 7 (b). The beam element length is set as 160.0 mm which corresponds to the thickness of the upper and lower flanges. In the other case, the beam element length is set as 216.5 mm, which includes the thickness of bolt head, nut and washers as well. The predicted axial bolt force with the applied force in Fig. 7 (c) shows good agreement with those from the study by Seidel and Schauman [26]. It is indicted that the beam bolt model can obtain accurate bolt axial forces and bending moments by choosing relevant beam length and the boundary condition of the top and bottom of the flange. The model and contact conditions for solid and beam models are summarized in Table 5.

The overview of tower top flange is shown in Fig. 3. The M24 bolt is modelled with the washer. The gravity centre of nacelle is in the rotor side, which generates a tension on the tower top flange and the bolts. ABAQUS is used for FEM analysis. The bird and sectional views of the nacelle are illustrated in Fig. 8 (a) and (b). The configuration and the sectional view of yaw drive as well as the detail of tower top are described in Fig. 8 (c) and (d). The nacelle connected with the tower with 120 ball bearings, 16 yaw breaks and 3 yaw motors supported by pinion gears. The yaw brakes break the nacelle rotation by pushing down the break plates with the spring force.

Table 2
Dimensions and weight of nacelle, hub, rotor, and tower.

Item	Unit	Value
Mass of nacelle	kg	39,000
Dimensions of the nacelle	m	3.3 (length) / 5.6 (width) / 6.5 (height)
Length of blade	m	23.35
Mass of rotor	kg	15,400
Hub height	m	50
Tower diameter	m	3.5 (bottom) / 2 (top)
Tower shell thickness	mm	16 (bottom) / 10 (top)
Damping ratio	%	0.5 (1st and 2nd mode)

Table 3
Tower structural characteristics.

	Measured (Hz)	Simulated (Hz)	Error
1st order (fore-aft) natural frequency	0.532	0.533	0.2 %
1st order (side-side) natural frequency	0.542	0.533	1.7 %
2nd order (fore-aft) natural frequency	3.838	3.685	4.0 %
2nd order (side-side) natural frequency	3.832	3.578	6.6 %

Table 4
Summary of identified control parameters.

	Unit	Standard PI	Pitch delay
Rated power	kW	630	630
Rotor speed	rpm	26	26
Error in pitch angle	degree	0	
Optimum power coefficient		0.3844	0.2980
Optimal mode gain	Nm/(rad/s^2)	30,361	23,537
Demanded generator torque	Nm	231,387	231,387
Torque control proportional gain		789,139	461,253
Torque control integral gain		516,780	176,554
Pitch control proportional gain		1.43422	0.65633
Pitch control integral gain		0.40213	0.76719
Gain scheduling for pitch control		Yoshida [25]	Yoshida [25]

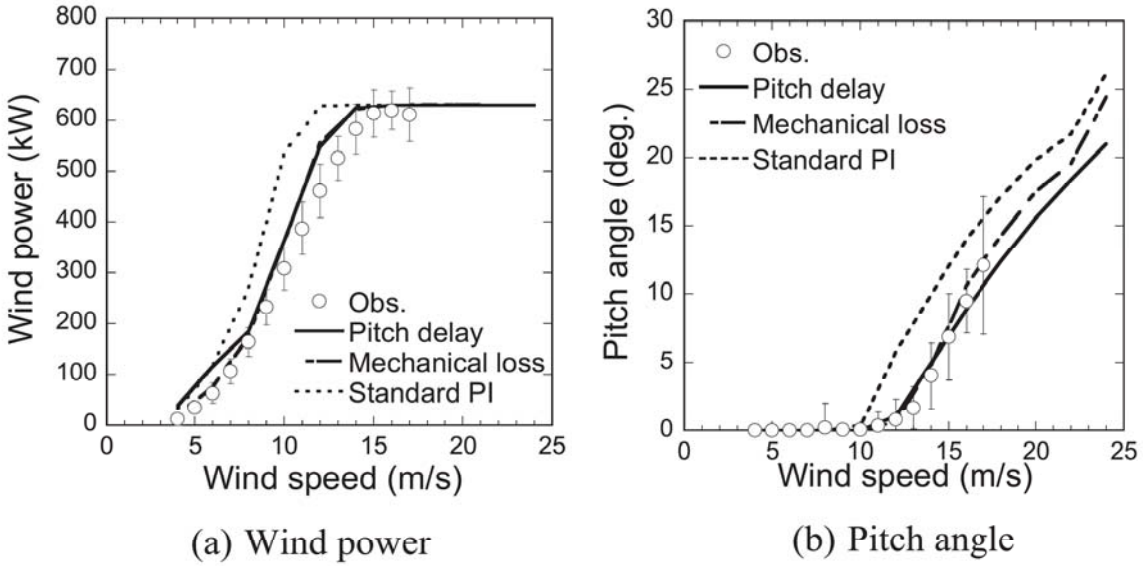

(a) Wind power (b) Pitch angle

Fig. 5. Comparison between measured and predicted power production and pitch angle.

The brake plate is jacked up when the nacelle is rotated. The yaw motors transfer the force through the gears as shown in Fig. 8 (e) and (f). The connection of the tower and the nacelle consists of L-shaped flanges with M24 bolts and washers.

The nacelle and yaw bearing at the tower top is modelled with three channels of ball bearings, yaw breaks and yaw pinion gears. The ball bearings are modelled as weak springs in Fig. 8 (c) because the acting loads are small in the parked condition. The yaw breaks are modelled by spring elements connected between the nacelle floor and yaw bearing blocks on the tower top, which represent the braking condition. The pinion gears are modelled by strong stiffness spring elements connecting pinion gears and yaw bearing blocks in Fig. 8 (f). The high-tension bolts are modelled by the beam elements considering the washer thickness and the bolt head thickness. Density is 7,850 kg/m3, Poisson's ratio is 0.3 and Young's modulus is 206,000 MPa. The FEM analysis is conducted in the elastic region. The bolt axial force is applied with initial stress. the nacelle self-weight considered as a concentrated force of 533,481 kN is then applied as statics load in the vertical direction. The measured material properties of the tower are used, but the flatness deviation of the upper and lower ring flange analysed by Seidel et al. [20], as well as the environmental factors such as temperature, humidity and corrosion are not considered in this study since these factors are not the root cause of the tower accident.

The predicted strain distributions on the tower shell at 20 mm below the tower-top flange by the rigid and elastic nacelle models are shown in Fig. 9. The predicted strain distribution by the elastic nacelle model reproduces the measured one, while those by the rigid nacelle model cannot catch the nonlinearity of the strain distribution.

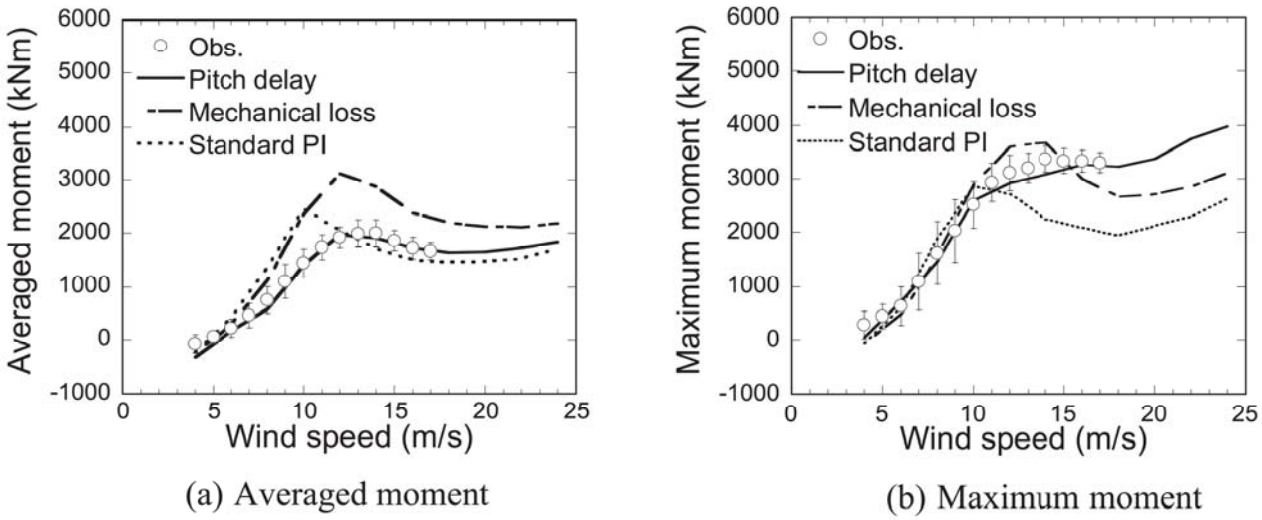

Fig. 6. Comparison between predicted and measured tower moment.

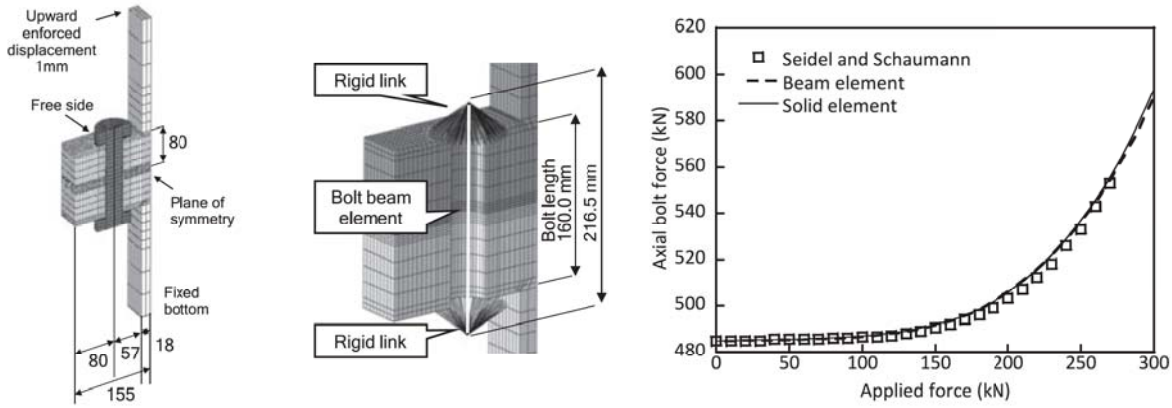

(a) Bolt solid element (b) Bolt beam element (c) Axial bolt forces

Fig.7. Numerical models for bolt connection and comparison of axial bolt forces by FEM models and Seidel and Schauman [26].

Table 5
Model and contact conditions for solid and beam models,

Description	Solid model	Beam model
Bolt	Solid element	Beam element
Flange	Solid element	Solid element
Washer	Solid element	Rigid
Model	1/2	Entire
Upper flange – lower flange	Contact	Contact
Flange-washer	Contact	Rigid connection
Flange-bolt	Contact	None

3. Results and discussions

Wind load on wind turbine tower is analysed in section 3.1. Fatigue analyses of high-tension bolts are conducted in section 3.2. Fatigue analyses of tower are performed in section 3.3.

3.1. *Wind load analysis on wind turbine tower*

The predicted wind load using the aeroelastic model are shown in Fig. 6. The axial stress N and bending moment M are evaluated at the tower top flange level at 45.94 m height above the ground. The tower nominal stress σ_N is calculated by Eq. (3).

(a) CAD drawing of nacelle

(b) Numerical model of nacelle

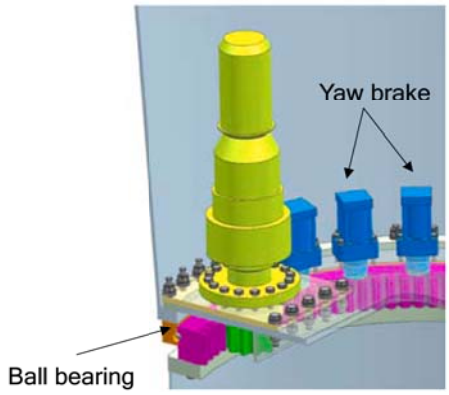

(c) CAD drawing of ball bearing and yaw break

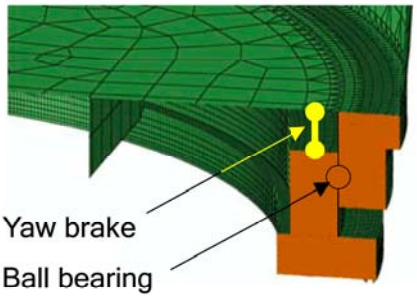

(d) Numerical model of ball bearing and yaw break

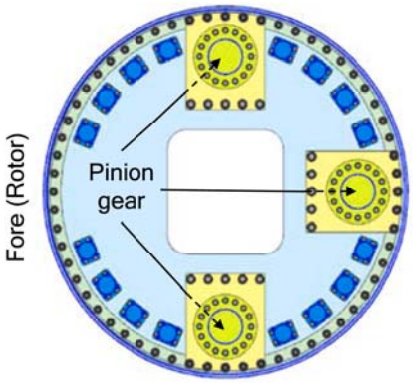

(e) CAD drawing of pinion gear

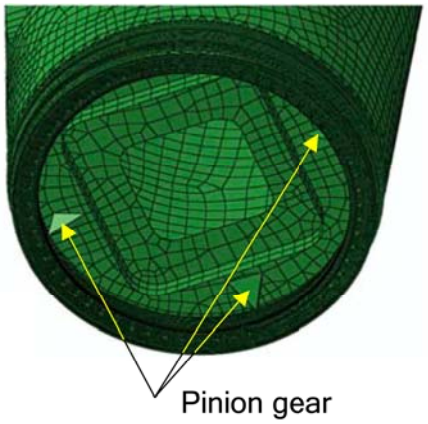

(f) Numerical model of pinion gear

Fig. 8. CAD drawings and numerical models of nacelle.

$$\sigma_N = \frac{N}{A} \pm \frac{M}{Z} \tag{3}$$

where A is the sectional area of fracture section of 0.062 m^2 and Z is the corresponding sectional modulus of 0.0309 m^3.

In Fig. 10 (a) and (b), the average values of axial force and bending moment in the case of no wind are −533 kN and −813 kNm respectively, which are induced by the rotor and nacelle self-weight. As the wind speed increases, the moment increases and reaches the maximum value near the rated wind speed. It is found that the moment on the tower due to the rotor and nacelle weight is larger than that due to the wind, which induces a tensile force at the downwind side of the tower. The nominal stresses are mostly positive due to the eccentric gravity force effect, but it becomes negative when the wind speed is higher than 18 m/s due to the wind loading as

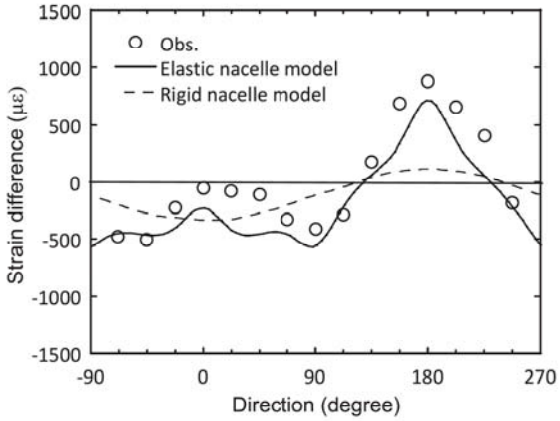

Fig. 9. Comparison of predicted and measured strains 20 mm below the tower-top flange.

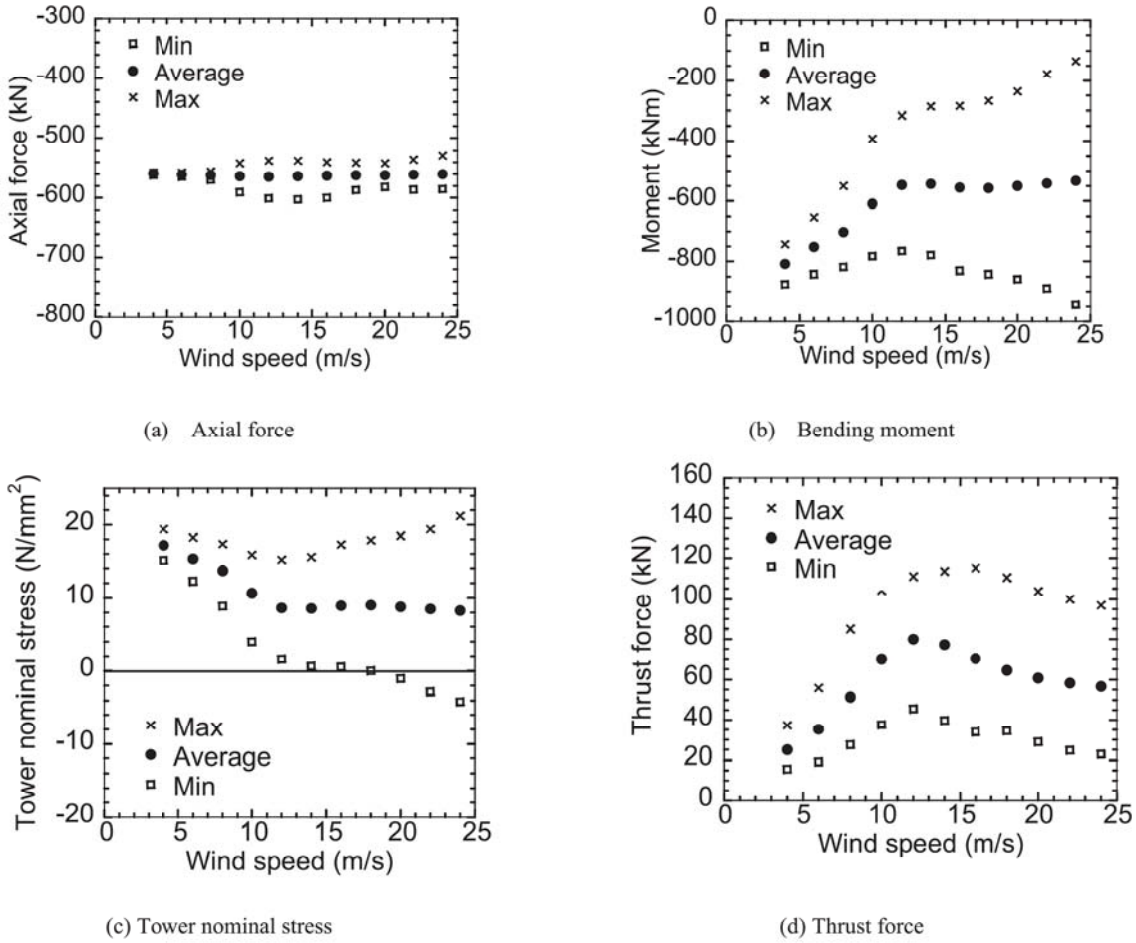

Fig. 10. Predicted maximum, average, and minimum wind loads on the tower.

shown in Fig. 10 (c). The nominal stress at the downwind side of tower is tensile at almost all the operational wind speed. This is the reason why the fatigue failure occurred at the downwind side of the tower. Fig. 10 (d) shows the thrust force acting on the tower top, which reaches the maximum value near the rated wind speed.

3.2. Fatigue analysis of high-tension bolts

The bolt axial stress of No. 3 wind turbine is calculated by using the full flange FEM model with various residual bolt axial forces. The bolt is modelled by a beam element as shown in Fig. 7 (b). The residual bolt axial force ratio is defined as the ratio of the residual

bolt axial force to the design pre-tension and is varied from 100 % to 0 % in the simulation. The design pre-tension of bolt is 265 kN in this study, which is 80 % of the material yield strength. The relationship between the bolt axial stress and tower nominal stress for different residual bolt axial force ratios is shown in Fig. 11. As the tower nominal stress increases, the slope of the curve increases because the contact force between the upper and lower flanges decreases. It is found that the flange opens faster as the residual bolt axial force ratio decreases. Fig. 12 shows the time series of bolt axial stress for two residual bolt axial force ratios based on the time series of wind loads at the hub height estimated by the aeroelastic wind turbine model. The variance of bolt axial stress in the case with 30 % residual bolt axial force ratio is much larger than that in the case with 80 % residual bolt axial force ratio.

The bolt fatigue life is analysed following the flowchart described in Fig. 13 (a). Dynamic analysis using the aeroelastic model considers blade rotation. The time series of the calculated moments and forces in six degrees of freedom by the aeroelastic model are used as the input of FEM model as shown in Fig. 3. The stress frequency distributions are calculated using the rainflow counted cyclic amplitudes from the simulated time series and Goodman correction. The S-N curve of ENV1993-1–1 Detail Category 50 [27] is used. The expected fatigue life is 21 years in the case with intact bolts for the residual axial force ratio of 80 %, while it decreases to 0.25 years in the case with damaged bolts for the residual axial force ratio of 30 % as shown in Fig. 13 (b). The maintenance records at the wind farm show that the bolt damages occurred in winter within about 1 to 3 months. The estimated fatigue life of 0.25 years using the wind condition in winter favourably agrees with the record. A possible mechanism for bolt failure is decrease of bolt axial force after replacing the yaw bearing or bolts as the flatness of the contact surfaces and bolt preload may change.

3.3. *Fatigue analysis of wind turbine tower shell*

Since the stress in the tower shell changes under different bolt tensions as shown by Kikuchi and Ishihara [16], the local stress in the tower shell is also investigated in this study using the tower top structural model for the intact bolt case and the damaged bolt case. Fig. 14 (a) shows a part of the tower top structural model. the case with damaged bolts, it is assumed that 17 bolts, No.13 to No.29, are failed based on the bolt maintenance record as shown in Table 1. The failure bolt is simulated by releasing the connection between the tower top flange and yaw bearing. The local stress is evaluated at the location of the maximum von Mises stress, which is observed on the east side of the tower in the intact bolt case, and 53.6 degrees from the east side of the tower in the damaged bolt case as shown in Fig. 2 (b). In the damaged bolt case, the top flange opens in the area where the bolts are failed and the wind loading is not transmitted to tower shell, so the local stress is concentrated at the end of the failed bolts. Fig. 14 (b) shows the stress counter of the tower top flange and tower shell in cases with the intact and damaged bolts. The maximum tensile stress is 84.6 N/mm^2 when the trust force is 50 kN and observed in the inside of tower shell, which can be explained by the leverage effect as shown in Fig. 15 (a). The tensile stress concentration inside tube coincides with the observation of fracture face.

The local stresses are estimated by the linear interpolation from the simulated stress values at 5 mm below the weld toe relative to the location where the crack occurred in the tower. Fig. 15 (b) shows that the relationship between the local stress and the tower nominal stress calculated by Eq. (3). It is found that the relationship between the local stress and the tower nominal stress is linear in the intact bolt case, but it is nonlinear in the damaged bolt case. The maximum local stress when the bolts were damaged becomes three times larger than that in the case with intact bolts.

The time series of the local stress on the tower shell is calculated using the relationship between the local stress and the tower nominal stress as shown in Fig. 15 (b). Similar to bolt fatigue life analysis, the rainflow counting and the Goodman relationship are used. The accumulated damage D is calculated using the S-N curve of tower shell and Miner's rule expressed as:

$$D = \sum_{i=1}^{k} \frac{n_i}{N_i} \leq 1 \tag{4}$$

where k is the number of different stress amplitudes and D is the accumulated damage within 20 years.

The evaluated fatigue life of No.3 wind turbine tower is shown in Table 6. In the case with intact bolts, the fatigue life is expected to be 42 years, corresponding to the annual damage of 0.024. When the bolts are damaged, the fatigue life reduces to 0.5 years,

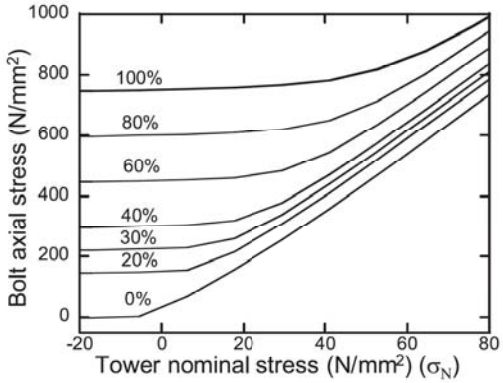

Fig. 11. Variation of bolt axial stress with tower nominal stress for different residual bolt axial force ratios.

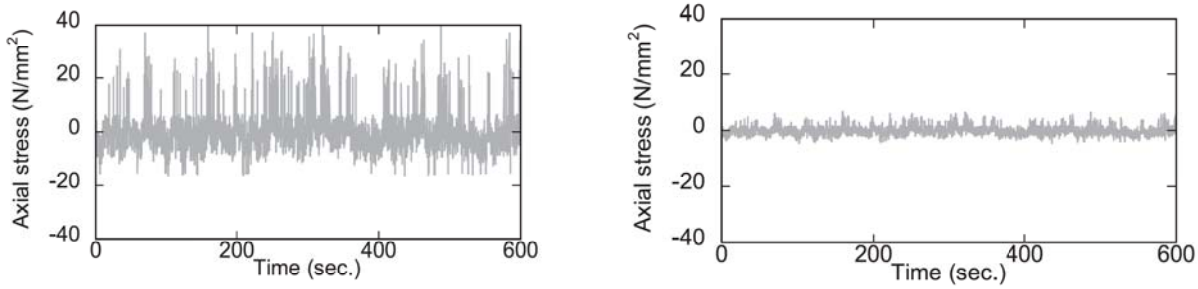

(a) 30% residual bolt axial force ratio (b) 80 % residual bolt axial force ratio

Fig. 12. Time series of predicted bolt axial stress for two residual bolt axial force ratios.

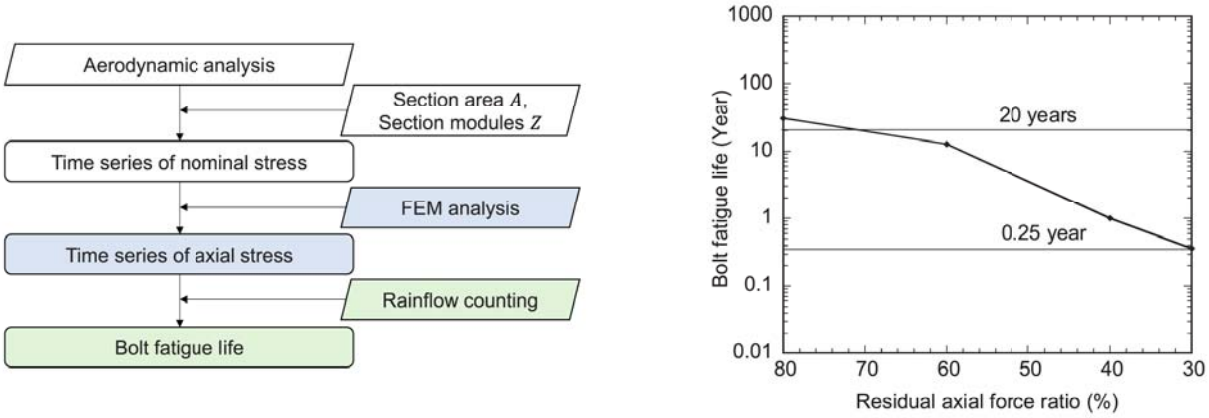

(a) Flowchart of bolt fatigue analysis (b) Bolt fatigue life

Fig. 13. Variation of bolt fatigue lifetime with residual bolt axial force ratio.

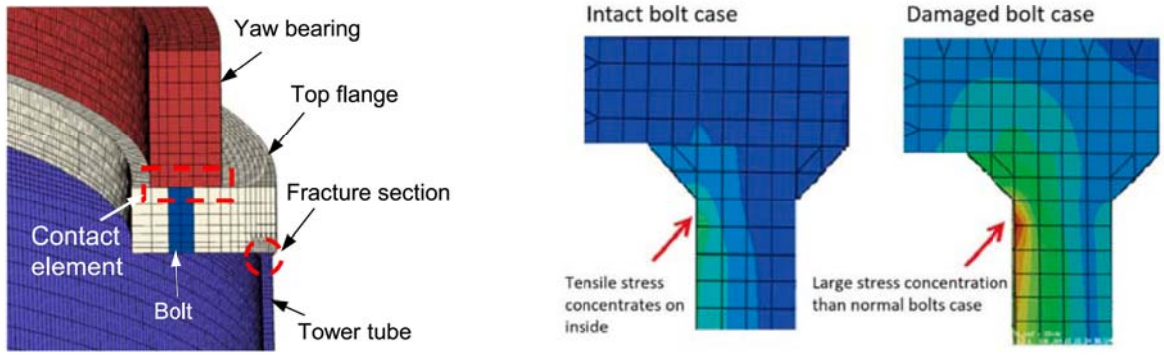

(a) Tower top structural model (b) Stress contour of the tower shell

Fig. 14. Comparison of stresses contours of the tower shell at the fracture section for cases with intact and damaged bolts.

corresponding to the monthly damage of 0.167. The durations of intact and damaged bolt cases are 11 years and 4–6 months obtained from the maintenance record as described in Table 1. The cumulative damage of the tower shell is predicted as 0.929 – 1.262. Considering the cumulative damage of tower shell in the case with intact bolts is 0.262, the average of cumulative damage of tower shell in the case with damaged bolts is estimated as 0.738, which corresponds to 4.42 months. This predicted fatigue life favorably agrees with the maintenance record of 4 to 6 months for wind turbine No.3.

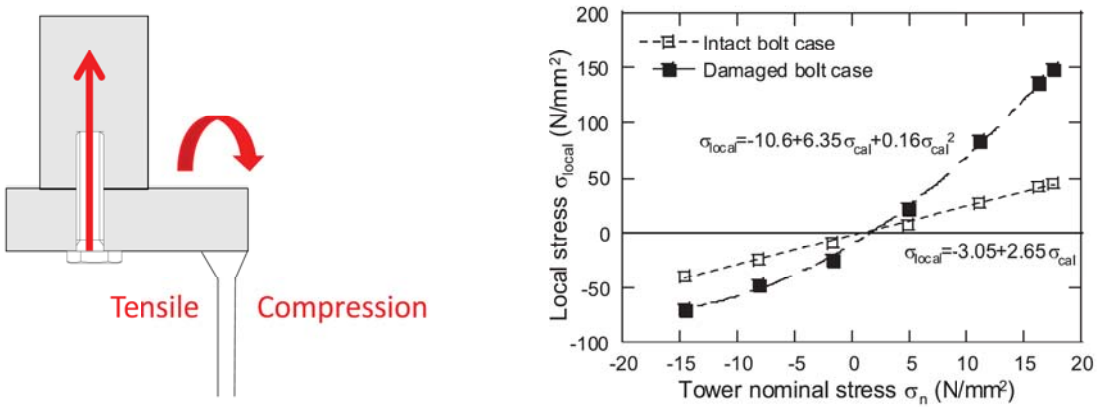

(a) Schematic of leverage effect (b) The local stress at the fracture section

Fig. 15. Comparison of local stresses at the fracture section for cases with intact and damaged bolts.

Table 6
Calculated fatigue life and damage for the intact and damaged bolt cases.

Case	Fatigue life	Damage	Duration	Cumulative damage
Intact	42 years	0.024/year	11 years	0.262
Damaged	0.5 years	0.167/month	4–6 months	0.667 – 1.000
Total				0.929 – 1.262

Based on the findings of this study, the high-tension bolts on the tower top flange of the existing wind turbines were replaced with bolts of a higher detail category, i.e. from hot-dip galvanized bolts with DC 50 to rolled after heat-treatment (RAHT) bolts with DC 85. The RAHT bolts have a longer fatigue life compared to hot-dip galvanized bolts due to the presence of compressive residual stresses on the surface as examined by Unglaub et al. [28]. After the replacement, no accidents occurred until the decommissioning of the wind farm. It indicates that choosing RAHT bolts has an advantage in fatigue life and the cost is not significantly different. Monitoring technology based on the relationship between tower stress and bolt axial force as shown in Kikuchi and Ishihara [16] are also useful. The optimization of the wind turbine tower design to mitigate its adverse effect has not been performed, which is considered as future work.

4. Conclusion

In this study, the fatigue life of wind turbine high-tension bolts and tower shell are predicted based on the aerodynamic and structural models and validated by the onsite measurements and the maintenance record. The following conclusions are obtained:

1) A sophisticated aeroelastic wind turbine model is proposed and the variation of wind load on the tower with wind speed is investigated. It is clarified that tensile stress occurs at the downwind side of the tower due to the eccentricity of the gravity centers of rotor and nacelle.
2) The bolt axial stress is predicted by the full flange FEM model. The predicted fatigue life of bolt with 30 % residual axial force is 0.25 years and agrees with the maintenance record of 1 to 3 months.
3) Based on the FEM analysis using a sophisticated structural model, it is revealed that the tensile stress is generated inside of the tower shell due to the leverage effect. The expected fatigue life of the tower with intact bolts is 42 years, while decreases to 0.5 years if bolts are damaged. The predicted fatigue life of the wind turbine tower with the damaged bolts agrees with the maintenance record of 4 to 6 months.

CRediT authorship contribution statement

Yuka Kikuchi: Writing – original draft, Visualization, Software, Investigation, Formal analysis, Data curation. **Takeshi Ishihara:** Writing – review & editing, Validation, Supervision, Resources, Methodology, Conceptualization.

Declaration of competing interest

The authors declare that they have no known competing financial interests or personal relationships that could have appeared to influence the work reported in this paper.

Acknowledgement

This study is carried out as a project funded by New Energy and Industrial Technology Development Organization. The authors wish to express their deepest gratitude to the concerned parties for their assistance during this study.

Data availability

The authors do not have permission to share data.

References

[1] Kyoto Prefecture, Report of Taikoyama Wind Farm No.3 Turbine Nacelle Collapse Accident, 2013. (In Japanese).
[2] K.-S. Lee, H.-J. Bang, A study on the prediction of lateral buckling load for wind turbine tower structures, Int. J. Precis. Eng. Manuf. 13 (2012) 1829–1836, https://doi.org/10.1007/s12541-012-0240-y.
[3] J.-S. Chou, W.-T. Tu, Failure analysis and risk management of a collapsed large wind turbine tower, Eng. Fail. Anal. 18 (2011) 295–313, https://doi.org/10.1016/j.engfailanal.2010.09.008.
[4] M. Alonso-Martinez, J. M. Adam, F. P. Alvarez-Rabanal, J. J. del Coz Díaz, Wind turbine tower collapse due to flange failure: FEM and DOE analyses, Eng. Failure Anal. 104 (2019) 932-949, DOI: 10.1016/j.engfailanal.2019.06.045.
[5] T. Tran, D. Lee, Understanding the behavior of l-type flange joint in wind turbine towers: Proposed mechanisms, Eng. Failure Anal. 142 (2022) 106750, https://doi.org/10.1016/j.engfailanal.2022.106750.
[6] A. Yamaguchi, P.W. Sarli, T. Ishihara, Extreme Load Estimation of the Wind Turbine Tower during Power Production, Wind Eng. (2019) 1–14, https://doi.org/10.1177/0309524X19872766.
[7] A. Yamaguchi, I. Yousefi, T. Ishihara, Reduction of the fluctuating load on wind turbine by using a combined nacelle acceleration feedback and Lidar-based feed-forward control, Energies 13 (2020) 4558, https://doi.org/10.3390/en13174558.
[8] T. Ishihara, S. Wang, Y. Kikuchi, Fatigue prediction of wind turbine main bearing based on field measurement and three-dimensional elastic drivetrain model, Eng. Failure Anal. 167 (2025) 108985, https://doi.org/10.1016/j.engfailanal.2024.108985.
[9] T. Ishihara, Y. Yoshimura, Y. Kenmochi, A Study on the Relationship between Tightening Torque and Axial Force of Bolts at the Tower Top Flange of Wind Turbine (In Japanese), Wind Energy 40 (2) (2016) 13–18, https://doi.org/10.11333/jwea.40.2_A_13.
[10] DEUTSCHE NORM, DIN 18800 Part 1 Structural steel work, Part 7 Execution and construction's qualification, 2002.
[11] VDI 2230 Blatt 1, Systematic calculation for high duty bolted joints, joints with one cylindrical bolt, 2003.
[12] Germanischer Lloyd, Guideline for the Certification of Wind Turbines; 2010.
[13] N.L. Pedersen, P. Pedersen, On prestress stiffness analysis of bolt-plate contact assemblies, Arch Appl Mech. 78 (2) (2008) 75–88, https://doi.org/10.1007/s00419-007-0142-0.
[14] N.L. Pederson, P. Pedersen, Bolt-plate contact assemblies with prestress and external loads: solved with super element technique, Comput Struct. 87 (21–22) (2009) 1374–1383, https://doi.org/10.1016/j.compstruc.2009.07.00419.
[15] J. Kang, H. Liu, D. Fu, Fatigue life and strength analysis of a main shaft-to-hub bolted connection in a wind turbine, Energies 12 (1) (2019) 7, https://doi.org/10.3390/en12010007.
[16] Y. Kikuchi, T. Ishihara, Anomaly Detection and Prediction for High-tension Bolts by Using Strain of Tower Shell, Wind Energy 23 (2020) 2186–2201, https://doi.org/10.1002/we.2551.
[17] H. Schmidt, M. Neuper, On the elastostatic behavior of an eccentrically tensioned L-joint with prestressed bolts, Stahlbau 66 (1997) 163–168. In German.
[18] NL. Pederson, On analysis and redesign of bolted L-flange connections. Wind Energy 20(6) (2017) 1069-1082, DOI: 10.1002/we.208020.
[19] I. Tobinaga, T. Ishihara, A study of action point correction factor for L-type flanges of wind turbine towers, Wind Energy 21 (9) (2018) 801–806, https://doi.org/10.1002/we.2193.
[20] M. Seidel, A. Stang, F. Wegener, C. Schierl, P. Schaumann, Full-scale validation of FE models for geometrically imperfect flange connections, J. of Constr. Steel Res., 187 (2021) 106955, https://doi.org/10.1016/j.jcsr.2021.106955.
[21] International Electrotechnical Commission, IEC 61400-12-1, Wind Turbines - Part 12-1: Power performance measurements of electricity producing wind turbines, 2005.
[22] Design Requirements (2019).
[23] T. Ishihara (ed.), Guidelines for Design of Wind Turbine Support Structures and Foundation. Japan Society of Civil Engineers (in Japanese), 2010.
[24] T. Burton, D. Sharpe, N. Jenkins (ed.), Wind Energy Handbook. John Wiley & Sons Ltd, Chichester, 115, 2011.
[25] S. Yoshida, Variable-speed Variable Pitch Control for Aero-servo-elastic Simulations of Wind Turbine Support Structures, J. Fluid Sci. Technol. 6 (2) (2011) 300–312, https://doi.org/10.1299/jfst.6.300.
[26] M. Seidel, P. Schaumann, Measuring fatigue loads of bolts in ring flange connections, Proceedings of European Wind Energy Association Conference, Copenhagen, Denmark 2001.
[27] Eurocode 3, Design of steel structures part1.1: General Rules and Rules for Buildings, 228, 1992.
[28] J. Unglaub, R.C. Wimpory, J. Hensel, In-depth residual stress analysis considering manufacturing process and cyclic loading of bolts, Eng. Struct. 267 (2022) 114652, https://doi.org/10.1016/j.engstruct.2022.114652.